

## Five-Wave-Mixing Spectroscopy of Ultrafast Electron Dynamics at a Si(001) Surface

C. Voelkmann, M. Reichelt, T. Meier, S.W. Koch, and U. Höfer

*Department of Physics and Material Sciences Center, Philipps University, Renthof 5, D-35032 Marburg, Germany*

(Received 11 September 2003; published 25 March 2004)

The optically induced electron dynamics at a Si(001) surface is studied using a five-wave-mixing setup which measures the diffracted second-harmonic intensity induced by three ultrashort (13 fs) laser pulses. Depending on the time ordering of the pulses, this technique is capable of monitoring the temporal evolution of photoexcited one- or two-photon coherences, or populations. For a particular pulse sequence, the experiments show a delayed rise and a decay of the diffracted signal intensity on time scales of 50 and 250 fs, respectively. This response can be described by optical Bloch equations by including rapid scattering of the photoexcited carriers in the  $D_{\text{down}}$  band of Si(001).

DOI: 10.1103/PhysRevLett.92.127405

PACS numbers: 78.47.+p, 42.65.Ky, 78.68.+m

The dynamics of excited states in condensed matter systems, atoms, and molecules has been studied extensively by optical techniques. In particular, time-resolved nonlinear optical spectroscopy in semiconductor systems using short laser pulses has provided valuable insight into the temporal evolution of particles and quasiparticles in nonequilibrium situations [1,2]. Compared to bulk or quantum well structures, the electron dynamics at semiconductor surfaces and interfaces is relatively poorly understood. The detailed mechanisms of carrier scattering and recombination at surfaces and interfaces is not only of great fundamental interest, it is also critical for the performance of modern small-scale devices. As of today, most of the experimental information has been obtained by time-resolved two-photon photoemission (2PPE) [3–5]. Because of its capability to determine energy and momentum of intermediate states, it is potentially more powerful than purely optical methods. Disadvantages of 2PPE are effects of transient band bending induced by the pump pulses that can severely limit the resolution at semiconducting surfaces. Moreover, the detection of electrons is generally restricted to high vacuum environments.

In this Letter, we introduce a new class of surface sensitive, time-resolved experiments that is complementary to 2PPE and avoids the aforementioned problems. We combine two well-established techniques: four-wave mixing (4WM) and second-harmonic generation (SHG). SHG, which is dipole forbidden in the bulk of centrosymmetric materials, and has become a very successful all-optical probe of surfaces and interfaces [6,7]. The combination, a five-wave-mixing (5WM) process, is able to deliver considerably more information than conventional pump and SHG-probe experiments [8,9]. In particular, it allows one to access the ultrafast coherent regime in a straightforward way just like 4WM in the bulk. We demonstrate the potential of the technique with results obtained for a Si(001) surface using ultrashort 13 fs pulses. The observed delayed rise and decay of the 5WM signal on time scales of 50 and 250 fs are both interpreted

in terms of scattering within the  $D_{\text{down}}$  band of the reconstructed surface. A simple model based on optical Bloch equations demonstrates that this response can be described by rapid scattering of the photoexcited carriers to other states in the momentum space of the surface which then dominantly contribute to the subsequently generated second harmonic.

In the 5WM experiment, we excite the sample with three ultrashort laser pulses of frequency  $\omega$  and measure the diffracted  $2\omega$  radiation generated by their nonlinear interaction at the surface. The three beams with wave vectors  $\mathbf{k}_a$ ,  $\mathbf{k}_b$ , and  $\mathbf{k}_c$  are incident in the  $x$ - $z$  plane ( $x$  denotes a direction parallel and  $z$  perpendicular to the surface). The  $2\omega$  signal is detected in a reflection geometry. To lowest order in the fields, its source is the fourth-order polarization:

$$\mathbf{P}_s^{(4)}(\mathbf{K}_d^{(+1)}, 2\omega) = \chi_s^{(4)} : \mathbf{E}_a^*(\mathbf{k}_a, \omega) \mathbf{E}_b(\mathbf{k}_b, \omega) \mathbf{E}_c^2(\mathbf{k}_c, \omega),$$

$$K_{d,x}^{(+1)} = 2k_{c,x} + (k_{b,x} - k_{a,x}). \quad (1)$$

Unlike 4WM which probes the third-order susceptibility  $\chi^{(3)}$  of the material,  $\chi_s^{(4)}$  is nonvanishing only for samples that lack inversion symmetry. For this reason 5WM, like SHG, is inherently surface specific in many situations.

It is instructive to view the 5WM process of Eq. (1) as SHG from a transient grating. The two pump beams  $a$  and  $b$  produce a population grating at the surface which gives rise to a spatial modulation of the second-order nonlinear susceptibility,  $\Delta\chi_s^{(2)}(x) = \Delta\chi_{s,0}^{(2)} \cos(k_G x)$ , with  $k_G = k_{b,x} - k_{a,x}$ . A fraction of the time-delayed probe beam  $c$  is frequency doubled and Bragg scattered from the grating into the direction  $\mathbf{K}_d^{(+1)}$ . The detected  $2\omega$  signal thus probes the modulation depth  $\Delta\chi_{s,0}^{(2)}$  of the grating as a function of the delay of beam  $c$ . It therefore contains information about carrier relaxation and carrier diffusion at the surface.

This simplified picture of the 5WM process is valid only for delays of beam  $c$  that are considerably longer than the durations of the exciting laser pulses and longer than the dephasing times of the system. In general,

several components that arise from the coherent interaction of the three beams contribute to the 5WM signal. By varying the time ordering of the pulses, the technique is thus capable of studying the temporal evolution of photo-excited one- and two-photon coherences.

The experiments were conducted with a cavity-dumped Ti:sapphire laser system [10] that delivered trains of 800 nm pulses at repetition rates from 100 kHz to 2 MHz with pulse durations of 13 fs and pulse energies up to 5 nJ. The *p*-polarized laser pulses were split with an intensity ratio of 1:1:2 and recombined on the sample at angles of 19°, 22°, and 27° with respect to the surface normal. The plane of incidence was normal to the [110] direction of Si(001); typical excitation fluences were 100  $\mu\text{J}/\text{cm}^2$ , which is only about 2% of the saturation intensity for the involved transitions. The 5WM signal was detected with a photomultiplier without polarization selection. The relative time delays between the three pulses were determined from the sum-frequency response of beams *a* and *b* and beams *b* and *c*, respectively. These signals are symmetric with respect to delay times and could be monitored simultaneously to the diffracted  $2\omega$  signal. All experiments were performed at clean well-ordered Si(001)- $c(4 \times 2)$  surfaces kept in ultrahigh vacuum at a temperature of 70 K. They were prepared by evaporating the native oxide from 10  $\Omega\text{ cm}$  P-doped Si wafers at 1300 K. By performing control experiments with oxygen covered surfaces, it was verified that the detected 5WM signal originates exclusively from the clean surface.

Representative data are plotted in Fig. 1(b) as functions of the delay time  $\tau_{ab}$  between the (pump) beams *a* and *b*. Different curves correspond to different delay time  $\tau_{bc}$  of (probe) beam *c* with respect to beam *b*. The delay times are referred to the time of incidence of pulse *b*; i.e., a pulse sequence *a, b, c* corresponds to  $\tau_{ab} < 0$  and  $\tau_{bc} > 0$ . For all delays  $\tau_{bc}$ , the  $2\omega$  response is sharply peaked and an almost symmetric function of  $\tau_{ab}$ . The full width at half maximum (FWHM) of 23 fs is similar to that of the sum-frequency signal from beams *a* and *b*. The FWHM of the latter is determined by the cross correlation of the two laser beams and the decay of the generated surface polarization. These results of the present three-beam 5WM experiment are similar to those of the self-diffraction data reported previously for Si(111)- $(7 \times 7)$  [11]. Whether the fast decay is a result of dephasing due to rapid scattering processes or has its origin in the destructive interference of a continuum of transition frequencies cannot be determined from the present experiment. In any case, the rapid decay as function of  $\tau_{ab}$  considerably simplifies the analysis of the temporal response of the 5WM signal as a function of delay time  $\tau_{bc}$ . In particular, it is possible to interpret the response measured for  $\tau_{bc} > 38$  fs (sum of pulse width and sum-frequency signal) as SHG from a transient population grating as described above.

In the following, we concentrate on the variation of the peak intensity on the delay of the probe beam *c*. For this

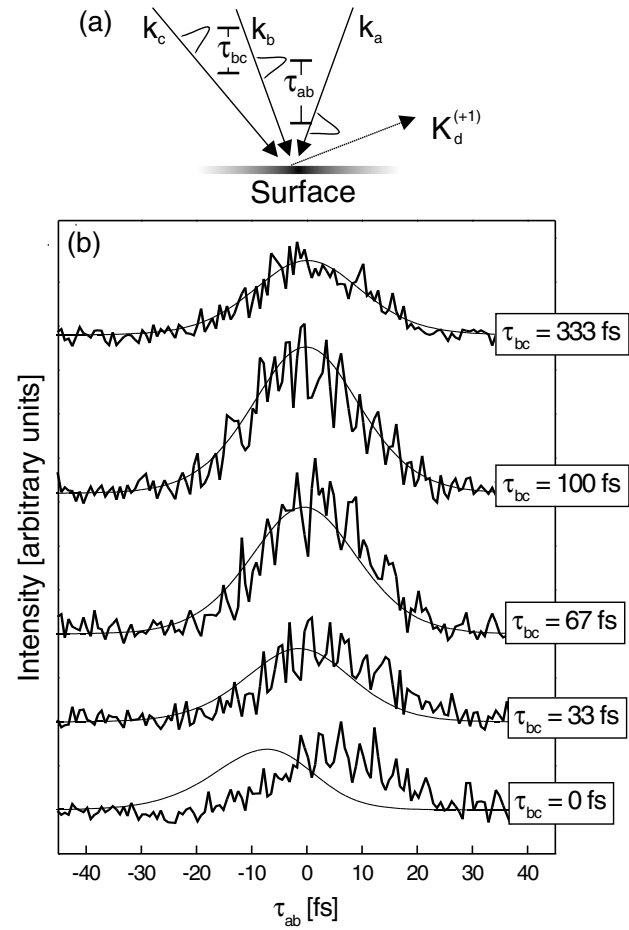


FIG. 1. (a) Geometry of the 5WM experiment using three temporally delayed incident beams *a*, *b*, and *c*. The second-harmonic signal is measured in the reflected direction  $\mathbf{K}_d^{(+1)}$ . (b) Time-integrated second-harmonic intensity as a function of  $\tau_{ab}$  for various  $\tau_{bc}$ . The thick solid lines are the measured transients and the thin lines display the results of the model calculations.

purpose, we plot in Fig. 2 the peak maxima from the data of Fig. 1(b) and from similar measurements as a function of  $\tau_{bc}$ . Surprisingly, the intensity does not show just a simple rise followed by a subsequent decay. Instead, after a sharp maximum around  $\tau_{bc} = 0$ , it goes through a minimum and reaches its absolute maximum at a delay of  $\sim 100$  fs and subsequently decays to zero on a time scale of  $T_1/2 = 250$  fs.

Whereas the sharp maximum at  $\tau_{bc} = 0$  can be understood to be the result of the coherent interaction of all three beams, the occurrence of a maximum, long after the two pump beams *a* and *b* are over, is unexpected. In a usual transient grating experiment, one expects that the grating modulation reaches its maximum near the end of the excitation pulses *a* and *b*. The maximum should therefore occur for a positive  $\tau_{bc}$  which is close to the duration of the pulses. For a short population relaxation time  $T_1$ , this maximum shifts even closer to delay zero since excitation and decay compete with each other. A shift towards large positive delays, as observed in Fig. 2,

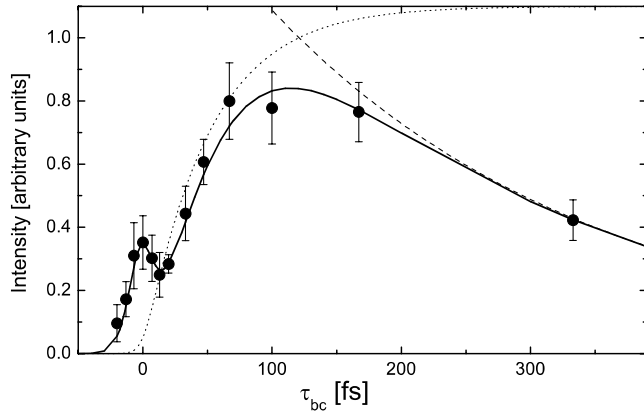


FIG. 2. Second-harmonic peak intensity, i.e., the maximum of the 5WM signal for varying  $\tau_{ab}$  but fixed  $\tau_{bc}$ , as a function of  $\tau_{bc}$ . The circles (with error bars) are the experimental results and the solid line displays the transient obtained from the model calculations. The dashed line denotes the long time limit, where the intensity is dominated by  $T_1$  processes and thus proportional to  $[\exp(-t/T_1)]^2$  with  $T_1 = 500$  fs. The dotted line displays the population on the lower one-photon resonance  $|1'\rangle$  of system  $S'$  (see Fig. 3) induced by a transfer time of  $T_{\text{trans}} = 50$  fs neglecting  $T_1$  processes.

requires some kind of transfer process between the generation of the grating and the probe of its properties.

In solid-state systems, a detailed interpretation of the optically induced dynamics requires an analysis of the interactions among the photoexcitations and with other quasiparticles. Microscopic theories describing this dynamics exist and have been successfully applied to conceptually simple systems such as direct semiconductors and semiconductor nanostructures within the framework of semiconductor Bloch equations [13]. Because of the overwhelming complexity of the interaction processes among surface and bulk states, similar microscopic theories for the time-resolved nonlinear optical response of surfaces are presently not available. Therefore, we use a Bloch equation description that phenomenologically incorporates known facts of the system to analyze the 5WM experiment.

With the photon energies of our laser systems of 1.55 eV, SHG from silicon is resonantly enhanced by dangling-bond derived surface states ( $1\omega$  resonance) and by surface-distorted bulk states ( $2\omega$  resonance near the  $E_1$  transition of bulk Si) [14–17]. In the case of Si(001), the dangling bonds are the  $D_{\text{up}}$  and  $D_{\text{down}}$  states of the asymmetric dimers. Resonant optical transitions from  $D_{\text{up}}$  to  $D_{\text{down}}$  are possible between the  $\bar{\Gamma}$  and  $\bar{J}'$  points of the surface Brillouin zone [Fig. 3(a)]. Since in this region of the dispersion the electrons are photoexcited well above the lowest energy of the  $D_{\text{down}}$  band, they will rapidly scatter towards lower energies and probably accumulate close to  $\bar{\Gamma}$  and/or  $\bar{J}'$ . This rapid relaxation process could be due to the emission of phonons associated with a flipping of the excited dimers and may also be accelerated by simultaneous Coulomb scattering processes.

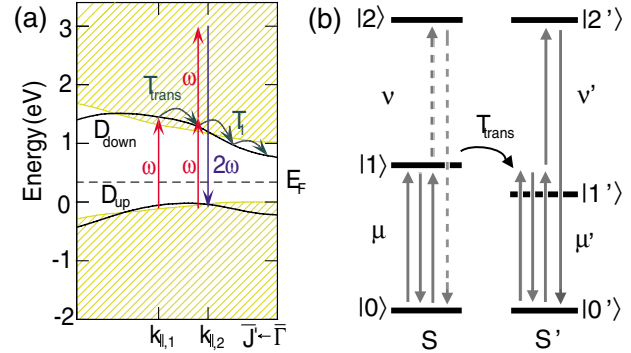


FIG. 3 (color online). (a) Band structure of Si(001)- $c(4 \times 2)$ , after Ref. [12]. (b) The two coupled three-level systems  $S$  and  $S'$  used in the numerical model calculations. Electronic relaxation from  $|1\rangle$  and  $|1'\rangle$  is modeled by a transfer time  $T_{\text{trans}}$ . The energy differences between  $|0\rangle$  and  $|2\rangle$  and  $|0'\rangle$  and  $|2'\rangle$  both coincide with twice the frequency of the incident beams.

Whereas in a standard degenerate 4WM experiment the excitation grating generated by beams  $a$  and  $b$  would be probed by beam  $c$  at the same  $k_{\parallel}$  value, this is generally not the case in a 5WM experiment. Here the probe which involves optical transitions at both  $\omega$  and  $2\omega$  is governed by different matrix elements than the pump. Especially in a situation where  $2\omega$  is close to a resonance, as in our experiment, it is possible to monitor the excitation grating at substantially different energies and momenta than created. Consequently, the temporal response of diffracted signal reflects both scattering *in* and *out* of the optically probed region. We emphasize, as matrix elements involving surface transitions are generally not well known, that it does not matter for our interpretation whether the electrons created in the  $D_{\text{down}}$  band originate from the  $D_{\text{up}}$  band or from bulklike states. Furthermore, the proposed excitation process is in agreement with recently performed 2PPE measurements by Weinelt *et al.* [18].

To substantiate our interpretation, we numerically solve optical Bloch equations for a model consisting of two coupled three-level systems  $S$  and  $S'$ ; see Fig. 3(b). The 5WM signal is calculated up to fourth order in the field by solving the equations of motion for the relevant polarizations, populations, and coherences, considering the finite duration of the exciting pulses. Dephasing and population relaxation are described by time constants  $T_2$  and  $T_1$ , respectively.

The calculated 5WM signals as a function of  $\tau_{ab}$  are shown by the thin lines in Fig. 1(b). For not too small  $\tau_{bc}$ , i.e., when the 5WM signal can be interpreted as a diffraction off a transient grating, the numerical results concerning the dependence on both  $\tau_{ab}$  and  $\tau_{bc}$  are in good agreement with experiment. For very small  $|\tau_{bc}|$  on the order of a few pulse widths, the numerical results are shifted as a function of  $\tau_{ab}$  relative to experiment. The origin of this temporal shift could be that our simple model does not include the continuum of off-resonant

transitions, three-photon resonances, and many-body interactions among the photoexcitations, which are known to lead to signals for positive  $\tau_{ab}$  in 4WM experiments [19] (note that the sign of  $\tau$  in [19] is reversed with respect to our definition of  $\tau_{ab}$ ). Since the main experimental feature we want to investigate is the delayed maximum observed in Fig. 2, the temporal shift between solid lines in Fig. 1(b) for very small  $|\tau_{bc}|$  is of no importance for the further analysis.

By calculating the SHG intensity as a function of  $\tau_{bc}$  for ensembles of independent (uncoupled) three-level systems, it is not possible to reproduce the delayed maximum of the experimental data of Fig. 2. As argued above, for this case the maximum of the SHG intensity appears at small positive  $\tau_{bc}$ . The delayed maximum can, however, be reproduced by considering a transfer process from level  $|1\rangle$  to level  $|1'\rangle$ . In more detail, for positive  $\tau_{bc}$  beams  $a$  and  $b$  resonantly create a strong population grating of  $|1\rangle$  and a much weaker off-resonant excitation at  $|1'\rangle$ . With increasing time, the population of  $|1\rangle$  is relaxing to  $|1'\rangle$ , which is modeled via a time constant  $T_{\text{trans}} = 50$  fs. For bulk silicon, 4WM experiments with 100 fs beams have revealed ultrafast dynamics on a time scale of  $\sim 10$  fs up to several 100 fs [20,21]. 2PPE experiments with 150 fs beams showed extremely rapid thermalization and cooling of photoexcited electrons ( $< 100$  fs) [4,5]. Therefore, the rapid time scale observed with our short 13 fs beams does not seem to be unreasonable. The fact that the delayed maximum is bigger than the initial one is reproduced by enhancing the transition matrix elements for the system  $S'$  in comparison to  $S$  in Fig. 3(b). This reduced model can be viewed to represent the most important transitions in the band structure. The system  $S$  corresponds to the value  $k_{\parallel,1}$  between  $\bar{\Gamma}$  and  $\bar{J}'$ . In this region, resonant single photon transitions to the  $D_{\text{down}}$  band, which is represented by  $|1\rangle$ , are expected. The system  $S'$  is situated at  $k_{\parallel,2}$  closer to the minimum of the  $D_{\text{down}}$  band, e.g., closer to the  $\bar{\Gamma}$  point.

Further results of our calculations are shown by the solid line in Fig. 2. Clearly, the experimental data are reproduced very well by the model. The long time limit is dominated by  $T_1$  processes; see dashed line in Fig. 2. The slow rise of the signal has its origin in the population transfer to  $|1'\rangle$ ; see dotted line. Qualitatively, the delayed maximum can be described by considering the product of the dashed and dotted lines.

In summary, the coherent optically induced dynamics at  $c(4 \times 2)$ -reconstructed Si(001) surfaces has been studied using a new class of five-wave-mixing (5WM) setup which measures the diffracted second-harmonic intensity induced by three femtosecond laser beams. Supported by model calculations based on optical Bloch equations, the observed ultrafast response was assigned to scattering of the excited electrons within the  $D_{\text{down}}$  surface band on time scales of 50–250 fs. In the future, similar 5WM experiments using more powerful, tunable

laser pulses will allow us to access the largely unexplored electron dynamics of buried semiconductor interfaces. Theoretically, more microscopic approaches will be developed to achieve a quantitative understanding of such time-resolved wave-mixing processes at surfaces and interfaces.

This work was funded by the Deutsche Forschungsgemeinschaft through HO2295/3, the Max-Planck Research program of the Humboldt and Max-Planck societies, and by the Center for Optodynamics, Philipps-University Marburg.

- 
- [1] D. S. Chemla and J. Shah, *Nature (London)* **411**, 549 (2001).
  - [2] *Ultrafast Physical Processes in Semiconductors, Semiconductors and Semimetals*, edited by K. T. Tseng (Academic, San Diego, 2001), Vol. 67.
  - [3] R. Haight, *Surf. Sci. Rep.* **21**, 275 (1995).
  - [4] J. R. Goldman and J. A. Prybyla, *Phys. Rev. Lett.* **72**, 1364 (1994).
  - [5] S. Jeong, H. Zacharias, and J. Bokor, *Phys. Rev. B* **54**, R17300 (1996).
  - [6] Y. R. Shen, *Annu. Rev. Phys. Chem.* **40**, 327 (1989).
  - [7] G. A. Reider and T. F. Heinz, in *Photonic Probes of Surfaces*, edited by P. Halevi (North-Holland, Amsterdam, 1995), pp. 3–66.
  - [8] H. W. K. Tom, G. D. Aumiller, and C. H. Brito-Cruz, *Phys. Rev. Lett.* **60**, 1438 (1988).
  - [9] J. Hohlfeld, S.-S. Wellershoff, J. Güdde, U. Conrad, V. Jähnke, and E. Matthias, *Chem. Phys.* **251**, 237 (2000).
  - [10] M. S. Pshenichnikov, W. P. de Boeij, and D. A. Wiersma, *Opt. Lett.* **19**, 572 (1994).
  - [11] C. Voelkmann, M. Mauerer, W. Berthold, and U. Höfer, *Phys. Status Solidi (a)* **175**, 169 (1999).
  - [12] J. Pollmann, P. Krüger, M. Rohlfing, M. Sabisch, and D. Vogel, *Appl. Surf. Sci.* **104/105**, 1 (1996).
  - [13] H. Haug and S. W. Koch, *Quantum Theory of the Optical and Electronic Properties of Semiconductors* (World Scientific, Singapore, 2004), 4th ed.
  - [14] W. Daum, H.-J. Krause, U. Reichel, and H. Ibach, *Phys. Rev. Lett.* **71**, 1234 (1993).
  - [15] U. Höfer, *Appl. Phys. A* **63**, 533 (1996).
  - [16] J. I. Dadap, Z. Xu, X. F. Hu, M. C. Downer, N. M. Russell, J. G. Ekerdt, and O. A. Aktsipetrov, *Phys. Rev. B* **56**, 13367 (1997).
  - [17] B. S. Mendoza, M. Palumbo, G. Onida, and R. D. Sole, *Phys. Rev. B* **63**, 205406 (2001).
  - [18] M. Weinelt, M. Kutschera, T. Fauster, and M. Rohlfing, *Phys. Rev. Lett.* **92**, 126801 (2004).
  - [19] K. Leo, M. Wegener, J. Shah, D. S. Chemla, E. O. Göbel, T. C. Damen, S. Schmitt-Rink, and W. Schäfer, *Phys. Rev. Lett.* **65**, 1340 (1990).
  - [20] R. Buhleier, G. Lüpke, G. Marowsky, Z. Gogolak, and J. Kuhl, *Phys. Rev. B* **50**, 2425 (1994).
  - [21] T. Sjödin, H. Petek, and H.-L. Dai, *Phys. Rev. Lett.* **81**, 5664 (1998).